

QCD results from the Fermilab Tevatron $p\bar{p}$ Collider

S. ROLLI

Tufts University - 4 Colby St, Medford, MA 02155, USA

(ricevuto il 14 Settembre 2010; pubblicato online il 5 Gennaio 2011)

Summary. — Several selected quantum chromodynamics (QCD) measurements performed at the Fermilab Tevatron by the CDF and D0 Collaborations, using proton-antiproton collisions at a centre-of-mass energy of $\sqrt{s} = 1.96$ TeV are reviewed. We will summarize the status of inclusive jet and dijet production cross-section measurements, which can be used to extract a precise value of the strong coupling constant and to search for physics beyond the Standard Model. We will then review results from the inclusive photon production cross-section measurement, as well as the associated production of photon with a light or heavy flavors jet. Finally we will describe various measurements concerning the production of vector bosons and jets.

PACS 14.80.Bn – Standard-model Higgs bosons.

1. – Introduction

Quantum chromodynamics (QCD), the theory of the strong interaction between quarks and gluons, is intrinsic to experimental studies of hadron collisions. This paper reviews several recent QCD results from the CDF and D0 experiments in analyses of $\sqrt{s} = 1.96$ TeV $p\bar{p}$ collisions. The general approach has been to test QCD theory, search for new physics phenomena, and enable electroweak and exotic measurements by informing Monte Carlo (MC) background models, while laying the groundwork for the LHC era of pp collisions.

2. – Inclusive jet production

The measurement of the differential inclusive jet cross section at the Fermilab Tevatron probes the highest momentum transfers in particle collisions currently attainable in any accelerator equipment, and thus is potentially sensitive to new physics such as quark substructure. The measurement also provides a direct test of predictions of perturbative quantum chromodynamics (pQCD). The inclusive jet cross section measurements at Tevatron Run II [1-4] cover up to 600 GeV/ c in jet transverse momentum p_T , and range over more than eight orders of magnitude in cross section. Comparisons of the measured

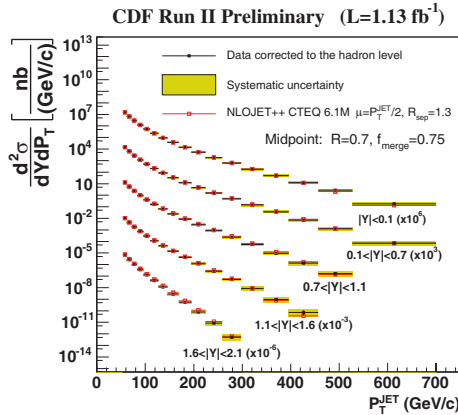


Fig. 1. – Inclusive jet cross section measured by CDF at the hadron level using the Midpoint algorithm in five rapidity regions compared with NLO pQCD predictions based on the CTEQ6.1M PDF. The cross sections for five rapidity regions are scaled by a factor of 10^3 from each other for presentation purposes.

cross section with pQCD predictions provide constraints on the parton distribution function (PDF) of the (anti)proton, in particular at high momentum fraction x ($x > 0.3$) where the gluon distribution is poorly constrained [5]. Further constraints on the gluon distribution at high x will contribute to reduced uncertainties on theoretical predictions of many interesting physics processes both for experiments at the Tevatron and for future experiments at the Large Hadron Collider (LHC). One example is $t\bar{t}$ production at the Tevatron for which the dominant PDF uncertainty arises from the uncertainty in the high- x gluon distribution. In addition, searches for new physics beyond the standard model at high p_T such as quark substructure require precise knowledge of PDFs at high x .

Both CDF [6] and D0 [7] measure the differential jet cross section using, respectively, 1.13 fb^{-1} and 0.70 fb^{-1} of data. Their measurements are in very good agreement with NLO predictions as can be seen in fig. 1 and fig. 2. The experimental precision now exceeds that of the PDF uncertainty, so that such measurements can be used, for the first time, to inform the PDF global fits.

3. – (α_s) measurement

Asymptotic freedom, the fact that the strong force between quarks and gluons keeps getting weaker when it is probed at increasingly small distances, is a remarkable property of quantum chromodynamics. This property is reflected by the renormalization group equation (RGE) prediction for the dependence of the strong coupling constant α_s on the renormalization scale μ_r and therefore on the momentum transfer. Experimental tests of asymptotic freedom require precise determinations of $\alpha_s(r)$ over a large range of momentum transfer. Frequently, α_s has been determined using production rates of hadronic jets in either e^+e^- annihilation or in deep-inelastic ep scattering (DIS). So far there exists only a single α_s result from inclusive jet production in hadron-hadron collisions. The CDF Collaboration determined α_s from the inclusive jet cross section in $p\bar{p}$ collisions at $\sqrt{s} = 1.8\text{ TeV}$ obtaining

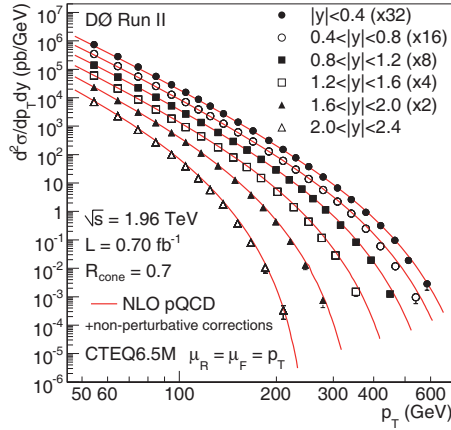


Fig. 2. – The inclusive jet cross section as a function of jet p_T in six $|y|$ bins, as measured by the D0 experiment. The data points are multiplied by 2, 4, 8, 16, and 32 for the bins $1.6 < |y| < 2.0$, $1.2 < |y| < 1.6$, $0.8 < |y| < 1.2$, $0.4 < |y| < 0.8$, and $|y| < 0.4$, respectively.

$\alpha_s(M_Z) = 0.1178 + 0.0081 \pm 0.0095$ (exp.) $+ 0.0071 \pm 0.0047$ (scale) ± 0.0059 (PDF) [8]. The D0 Collaboration has recently determined α_s and its dependence on the momentum transfer using the published measurement of the inclusive jet cross section with the D0 detector at the Fermilab Tevatron Collider in $p\bar{p}$ collisions at $\sqrt{s} = 1.96$ TeV [9]. The measurement used the p_T dependence of the jet cross section and is obtained by minimizing a χ^2 between data and theory (NLO plus two-loop thresholds corrections), where 22 points out of 110 from the jet inclusive cross section are used in the p_T range 50–145, and excluding high- p_T points to minimize PDF uncertainty correlations. A combined fit to all 22 data points yields $\alpha_s(M_Z) = 0.1161 + 0.0041 - 0.0048$ with $\chi^2/\text{ndf} = 17.2/21$. The $\alpha_s(p_T)$ results support the energy dependence predicted by the renormalization group equation. This is the most precise α_s result obtained at a hadron collider.

4. – dijet production

Within the standard model (SM), two-jet (dijet) events are produced in proton-antiproton collisions predominantly from hard quantum chromodynamics (QCD) interactions of two partons. The fragmentation and hadronization of the outgoing partons produce hadronic jets. The dijet mass spectrum predicted by QCD falls smoothly and steeply with increasing dijet mass. Many extensions of the SM predict the existence of new massive particles that decay into two energetic partons (quarks, q , or gluons, g), which can potentially be observed as a narrow resonance in the dijet mass spectrum. Such particles include excited quarks, axigluon, flavor-universal coloron, color-octet techni- ρ , Randall-Sundrum (RS) graviton, W' , Z' and diquark in the string-inspired E6 model. CDF [10] and D0 [11] are both measuring the dijet mass distribution.

In the CDF result, the measured dijet mass spectrum is compared to the next-to-leading-order perturbative QCD (NLO pQCD) predictions from fastNLO [12]. The predictions were obtained using the CTEQ6.1 PDFs with the renormalization and factorization scales both set to μ_0 , the average p_T of the leading two jets. The data and theoretical predictions are found to be in good agreement. CDF then searches for narrow mass res-

onances in the measured dijet mass spectrum by fitting the measured spectrum to a smooth functional form and by looking for data points that show significant excess from the fit. No evidence for the existence of a resonant structure is found and limits on new particle production (W' , Z' , RS graviton, excited quarks) are set (see ref. [10]).

5. – Limits on new physics from dijets measurements

The angular distribution of dijets with respect to the hadron beam direction is directly sensitive to the dynamics of the underlying reaction. While in quantum chromodynamics (QCD) this distribution shows small but noticeable deviations from Rutherford scattering, an excess at large angles from the beam axis would be a sign of new physics processes not included in the SM, such as substructure of quarks (*quark compositeness*), or the existence of additional compactified spatial dimensions (*extra dimensions*). D0 performs a measurement of the variable $\chi_{\text{dijets}} = \exp[|y_1 - y_2|]$ in ten regions of dijet invariant mass M_{jj} , where y_1 and y_2 are the rapidities of the two jets with highest transverse momentum p_T with respect to the beam axis in an event. For massless $2 \rightarrow 2$ scattering, the variable χ_{dijet} is related to the polar scattering angle θ^* in the partonic center-of-mass frame. The choice of this variable is motivated by the fact that Rutherford scattering is independent of χ_{dijet} , while new physics shows an enhancement at low values of the variable. This is the first measurement of angular distributions of a hard partonic scattering process at energies above 1 TeV in collider-based high energy physics. The normalized χ dijet distributions are well described by theory calculations in next-to-leading order in the strong coupling constant and are used to set limits on quark compositeness, ADD large extra dimensions, and TeV^{-1} extra dimensions models. For the TeV^{-1} extra dimensions model this is the first direct search at a collider. For all models considered, this analysis sets the most stringent direct limits to date (see table in ref. [13]).

6. – Inclusive photon production

Photons originating in the hard interaction between two partons are typically produced in hadron collisions via quark-gluon Compton scattering or quark-anti-quark annihilation. Studies of these direct photons with large transverse momenta, p_T , provide precision tests of perturbative QCD (pQCD) as well as information on the distribution of partons within protons, particularly the gluon. These data were used in global fits of parton distributions functions (PDFs) and complement analyses of deep inelastic scattering, Drell-Yan pair production, and jet production. Photons from energetic π^0 and η mesons are the main background to direct photon production especially at small p_T . Since these mesons are produced inside jets, their contribution can be suppressed with respect to direct photons by requiring the photon be isolated from other particles. Isolated electrons from the electroweak production of W and Z bosons also contribute to the background at high p_T . Several measurements of photon production at hadron colliders successfully used these isolation techniques to extract the photon signal.

Both CDF [14] and D0 [15] have measured the cross-section for inclusive production of isolated photons. Results from NLO pQCD calculations agree with the measurement within uncertainties. The ratio between data and pQCD prediction is in good agreement at high p_T but shows an enhancement at low p_T where the effects of theory resummation and background fragmentation are higher.

7. – Production of photon in association with jets

7.1. Photon + jet. – The production of a photon with associated jets in the final state is a powerful probe of the dynamics of hard QCD interactions. Different angular configurations between the photon and the jets can be used to extend inclusive photon production measurements and simultaneously test the underlying dynamics of QCD hard-scattering subprocesses in different regions of parton momentum fraction x and large hard-scattering scales Q^2 .

At D0 [16], the process $p\bar{p} \rightarrow \gamma + \text{jet} + X$ is studied using 1.0 fb^{-1} of data. Photons are reconstructed in the central rapidity region $|y_\gamma| < 1.0$ with transverse momenta in the range $30 < p_T^\gamma < 400 \text{ GeV}$ while jets are reconstructed in either the central $|y_{\text{jet}}| < 0.8$ or forward $1.5 < |y_{\text{jet}}| < 2.5$ rapidity intervals with $p_T^{\text{jet}} > 15 \text{ GeV}$. The differential cross section $d^3\sigma/dp_T^\gamma dy_\gamma dy_{\text{jet}}$ is measured as a function of p_T^γ in four regions, differing by the relative orientations of the photon and the jet in rapidity. Ratios between the differential cross sections in each region are also presented. Next-to-leading order QCD predictions using different parameterizations of parton distribution functions and theoretical scale choices are compared to the data. The predictions do not simultaneously describe the measured normalization and p_T^γ dependence of the cross section in the four measured regions. Similarly, theoretical scale variations are unable to simultaneously describe the data-to-theory ratios in each of the four measured regions. Thus, the data show a need for an improved and consistent theoretical description of the $\gamma + \text{jet}$ production process.

7.2. Photon + heavy flavor jets. – Photons (γ) produced in association with heavy quarks Q (c or b) in the final state of hadron-hadron interactions provide valuable information about the parton distributions of the initial state hadrons. Such events are produced primarily through the QCD Compton-like scattering process $gQ \rightarrow \gamma Q$, which dominates up to photon transverse momenta (p_T^γ) of 90 GeV for $\gamma + c + X$ and up to 120 GeV for $\gamma + b + X$ production, but also through quark-antiquark annihilation. Consequently, $\gamma + Q + X$ production is sensitive to the b , c , and gluon (g) densities within the colliding hadrons, and can provide constraints on parton distribution functions (PDFs) that have substantial uncertainties. The heavy quark and gluon content is an important aspect of QCD dynamics and of the fundamental structure of the proton. In particular, many searches for new physics, *e.g.*, for certain Higgs boson production modes, will benefit from a more precise knowledge of the heavy quark and gluon content of the proton.

First measurements of the differential cross sections $d^3\sigma/(dp_T^\gamma dy_\gamma dy_{\text{jet}})$ for the inclusive production of a photon in association with a heavy quark (b , c) jet are presented by D0 [17], covering photon transverse momenta $30 < p_T^\gamma < 150 \text{ GeV}$, photon rapidities $|y_\gamma| < 1.0$, jet rapidities $|y_{\text{jet}}| < 0.8$, and jet transverse momenta $p_T^{\text{jet}} > 15 \text{ GeV}$. The results are compared with next-to-leading order perturbative QCD predictions. The pQCD prediction agrees with the measured cross sections for $\gamma + b + X$ production over the entire p_T^γ range, and with $\gamma + c + X$ production for $p_T^\gamma < 70 \text{ GeV}$. For $p_T^\gamma > 70 \text{ GeV}$ the measured $\gamma + c + X$ cross section is higher than the prediction by about 1.6 to 2.2 standard deviations (including only the experimental uncertainties) with the difference increasing with growing p_T^γ as shown in fig. 3.

8. – Vector boson + jets production

Collider signatures containing bosons and jets are particularly interesting. Recent theoretical effort has been devoted to determining predictions of $W^\pm/Z + \text{multiple parton}$

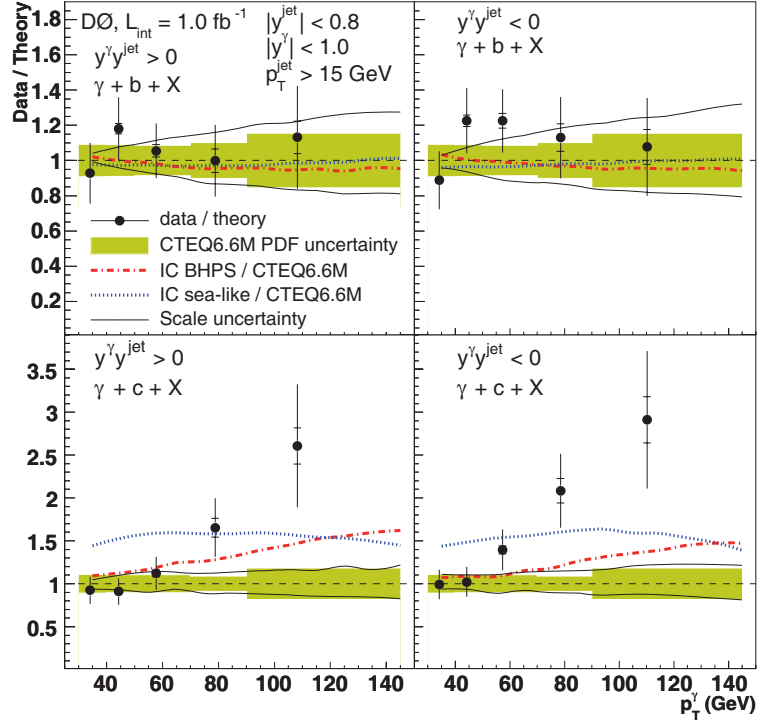


Fig. 3. – The data-to-theory ratio of cross sections as a function of p_T^γ for $\gamma+b+X$ and $\gamma+c+X$ in the regions $y^\gamma y^{\text{jet}} > 0$ and $y^\gamma y^{\text{jet}} < 0$. The uncertainties on the data include both statistical (inner line) and full uncertainties (entire error bar). Also shown are the uncertainties on the theoretical pQCD scales and the CTEQ6.6M PDFs. The scale uncertainties are shown as dotted lines and the PDF uncertainties by the shaded regions. The ratio of the standard CTEQ6.6M prediction to two models of intrinsic charm is also shown.

production; the high-statistics sample of $W^\pm/Z + \text{jets}$ events collected at the Tevatron is a valuable testbed for probing the validity of these calculations. The final state containing a Z or W boson and one or more b-jets is a promising Higgs search channel at the Tevatron and could be a window to new physics at the LHC. These searches benefit from a deep understanding of the production of $W^\pm/Z + \text{heavy flavor jets}$ which constitutes a significant background to the more exotic sources of this signature. In this section the latest Tevatron results on these production mechanisms are reviewed with an emphasis on comparison of data results to the latest theoretical models.

8.1. $W/Z + \text{jets}$. – The CDF experiment has studied the production of jets in events with W^\pm/Z bosons [18,19]. $W \rightarrow e\nu$ events are selected by identifying a high E_T , central electron along with significant missing transverse energy, MET; $Z \rightarrow e^+e^-$ events are selected by requiring one such electron with another that is either central or in the forward region of the calorimeter, with the invariant mass of the electron pair required to be near the Z mass peak. Events are then assigned to bins of minimum jet multiplicity. Major sources of background in the $W^\pm + \text{jets}$ analysis include events with fake Ws and electroweak sources (tt, single top, dibosons); backgrounds in the $Z + \text{jets}$ analysis are dominated by multijet production and $W^\pm + \text{jets}$ events in which the Z signal is faked.

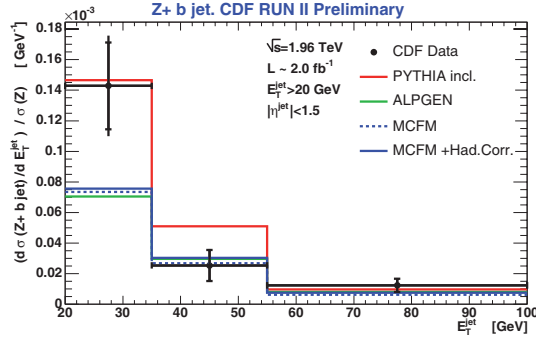


Fig. 4. – $Z + b$ jet differential cross sections as a function of jet p_T from CDF's 2 fb^{-1} result.

Acceptance for these events is studied using simulated signal samples; the differential cross section for the jets in these events is then examined and compared to some available theory predictions. NLO prediction from MCFM is accurately reproducing the jet E_T spectrum in $W^\pm + 1$ or 2 jets. For higher multiplicity events, LO calculations are only available. The current preferred method for generating such events at LO relies on generating multiple samples using a matrix element calculation at fixed orders in α_s and then employing a parton shower program to add in additional soft, collinear jets. Matching algorithms have been designed to identify events that could be double counted in this recipe.

8.2. $Z + \text{jets}$ angular distributions. – A recent measurement by D0 of the inclusive cross section for $Z/\gamma^*(\rightarrow e^+e^-) + \text{jets}$ [20] tests NLO pQCD and provides an important control on background to new physics. Events are binned in the p_T of the N -th jet, for $N = 1, 2$, and 3. Data agree well with NLO-MCFM but diverge from predictions by PYTHIA and HERWIG increasingly with jet p_T and N_{jet} . PYTHIA with p_T ordering is found to describe the leading jet well. SHERPA and ALPGEN are seen to improve upon the particle shower-based generators. Some discrepancies persist nonetheless between data and predictions of production rates and jet p_T spectra.

8.3. $W + \text{single-}c$ production. – $W + \text{single-}c$ production is an important process at the Tevatron. $W + \text{single-}c$ events are produced via gluon-strange quark scattering, and thus this process offers insight on the strange content inside the proton. The process also allows an opportunity to measure $|V_{cs}|$ in a Q^2 regime not yet probed. Also, $W + c$ contributes to the background to top production and prominent Higgs search channels at the Tevatron. CDF [21] and D0 [22] have measured the $W + c$ process in Run II using a similar strategy. Leptonic W decays ($W \rightarrow l\nu$ with $l = e$ or μ) are selected via a high- p_T isolated central lepton and large missing E_T . Among the required jets in the selected events, evidence is sought for semileptonic hadron decay through the identification of a soft muon inside the jet cone. It is a feature of $W + c$ production that the electric charge of the W and c are opposite. The sign of the c quark is determined from the charge of the muon used to identify semileptonic hadron decay. An excess of opposite-sign primary lepton and soft muon events is indicative of $W + c$ production. Opposite-sign backgrounds include Drell-Yan production of $\mu^+\mu^-$, Wq production and fake W s. CDF measured in 1.7 fb^{-1} of data the production cross section for $W + c$ times the leptonic branching ratio of the W , $\sigma(Wc)BR(W \rightarrow l\nu) = 9.8 + 3.2$ for events with $p_T^c > 20 \text{ GeV}/c$ and

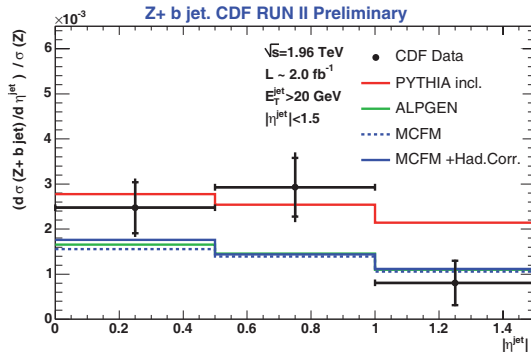


Fig. 5. – Z + b jet differential cross sections as a function of jet η from CDFs 2 fb^{-1} result.

$|\eta| < 1.5$. This can be compared to the NLO prediction from MCFM of $11.0^{+1.4}_{-3.0}$. D0 measured in 1 fb^{-1} of data the ratio $R = \frac{\sigma(Wc)}{\sigma(W+\text{jets})}$; measuring the ratio has the virtue that numerous sources of systematic error cancel out. The result $R = 0.071 \pm 0.017$ is reasonably consistent with a LO prediction from ALPGEN of 0.040 ± 0.003 .

8.4. $W^\pm/Z + b$ jets. – $W^\pm/Z + b$ jet signatures are important backgrounds to top and Higgs channels at the Tevatron. Separate analyses were undertaken to measure the b-jet cross section in W^\pm and Z events with increased precision in the hopes of improving the understanding of these final states. The event selection for the $W^\pm + b$ jets analysis is similar to that employed in the $W + c$ analysis discussed above. Here however b-jets are selected via the identification of a secondary decay vertex well separated from the primary $p\bar{p}$ interaction point.

The b-jet cross section in W^\pm events in 1.9 fb^{-1} of CDF Run II data was measured to be $\sigma + b - \text{jets}(W + b + \text{jets})BR(W \rightarrow l\nu) = 2.74 \pm 0.27(\text{stat}) \pm 0.42(\text{syst}) \text{ pb}$, where the systematic error is dominated by the uncertainty in the vertex mass shape one assumes for b-jets. This jet cross section result can be compared to the prediction from ALPGEN of 0.78 pb , a factor of 3-4 lower than what is observed in the data. Work is ongoing to understand the difference.

The Z+b-jet analysis used a similar technique to extract the b content of its tagged jet sample. This analysis has succeeded in examining differential cross sections for the b-jets in Z events as shown in fig. 4 and fig. 5. One can see that the differential b-jet cross sections *versus* jet p_T and η are not reproduced in all bins by any of the predictions that were constructed. Pythia appears to do a reasonable job at low jet p_T but less so as the jet p_T increases. The ALPGEN and MCFM predictions are consistent with each other but not with the data except for a few bins. It remains to be understood why the predictions are so different.

9. – Conclusions

We have reported on selected recent quantum chromodynamics (QCD) measurements from the Fermilab Run II Tevatron proton-antiproton collisions studied by the CDF and D0 Collaborations at a centre-of-mass energy of $\sqrt{s} = 1.96 \text{ TeV}$. We have reviewed inclusive jet and dijet production cross-section measurements, which are in excellent agreement with the theoretical predictions and are now being used for the first time

to inform parton distribution functions (PDF) determination. Jet and dijets measurements are also used to extract a precise value of the strong coupling constant and to look for new physics. Results from the inclusive photon production cross-section measurement, as well as associated production of photon with a light or heavy flavors jet, reveal still an inability of the next-to-leading-order (NLO) perturbative QCD calculations to describe comprehensively all such measurements. Finally we have summarized various measurements concerning the production of vector bosons and jets. Such measurements are a common prerequisite for many other studies, from top production measurements to search for supersymmetric particles and the Higgs boson. Several pQCD NLO calculations are now becoming available as well as several Monte Carlo tools, which can be validated against such experimental measurements.

REFERENCES

- [1] ABULENCIA A. *et al.*, *Phys. Rev. D*, **74** (2006) 071103.
- [2] ABULENCIA A. *et al.*, *Phys. Rev. Lett.*, **96** (2006) 122001.
- [3] ABULENCIA A. *et al.*, *Phys. Rev. D*, **75** (2007) 092006.
- [4] ABAZOV V. M. *et al.*, *Phys. Rev. Lett.*, **101** (2008) 062001.
- [5] STUMP D. *et al.*, *J. High Energy Phys.*, **10** (2003) 046.
- [6] ALTOONEN T. *et al.*, *Phys. Rev. D*, **78** (2008) 052006.
- [7] ABAZOV V. M. *et al.*, *Phys. Rev. Lett.*, **101** (2008) 062001.
- [8] CDF COLLABORATION, *Phys. Rev. Lett.*, **88** (2002) 042001.
- [9] ABAZOV V. M. *et al.*, *Phys. Rev. D*, **80** (2009) 111107.
- [10] CDF COLLABORATION, *Phys. Rev. D*, **79** (2009) 112002.
- [11] D0 COLLABORATION, arXiv.org:1002.4594.
- [12] KLUGE T., RABBERTZ K. and WOBISCH M., arXiv:hep-ph/0609285 (2006).
- [13] ABAZOV V. M. *et al.*, *Phys. Rev. Lett.*, **103** (2009) 191803.
- [14] <http://www-cdf.fnal.gov/physics/new/qcd/inclpho08/web.html>
- [15] ABAZOV V. M. *et al.*, *Phys. Lett. B*, **639** (2006) 151.
- [16] ABAZOV V. M. *et al.*, *Phys. Lett. B*, **666** (2008) 435.
- [17] ABAZOV V. M. *et al.*, *Phys. Rev. Lett.*, **102** (2009) 192002.
- [18] AALTONEN T. *et al.*, *Phys. Rev. D*, **77** (2008) 011108R.
- [19] AALTONEN T. *et al.*, *Phys. Rev. Lett.*, **100** (2008) 102001.
- [20] ABAZOV V. M. *et al.*, *Phys. Lett. B*, **678** (2009) 45.
- [21] AALTONEN T. *et al.*, *Phys. Rev. Lett.*, **100** (2008) 091803.
- [22] ABAZOV V. M. *et al.*, *Phys. Lett. B*, **666** (2008) 23.